ELSEVIER

Polymer 42 (2001) 2241–2245

polymer

www.elsevier.nl/locate/polymer

Polymer Communication

Morphology and crystal structure of cold-crystallized syndiotactic polystyrene

Y.S. Sun, E.M. Woo*

Department of Chemical Engineering, National Cheng Kung University, Tainan 701-01, Taiwan

Received 6 June 2000; received in revised form 22 July 2000; accepted 28 July 2000

Abstract

Scanning electron microscopy, differential scanning calorimetry, IR spectroscopy, and X-ray diffraction analyses were used to characterize the unique morphology of cold-crystallized syndiotactic polystyrene (sPS). Cold-crystallization of sPS produced only α-type unit cell packed into crystalline domains of different morphologies. The morphology contains a granular-sphere texture when cold-crystallized at low temperatures while high-temperature cold-crystallization produced additional sheaf-like lamella radiating out from the central spheres. Details of this interesting morphological feature are expounded in the paper. © 2000 Elsevier Science Ltd. All rights reserved.

Keywords: Cold-crystallization; Syndiotactic polystyrene; Crystal form

1. Introduction

Most semicrystalline polymers possess only one type of crystal unit cell, but some others may possess polymorphism with different chain-packing crystals. Interestingly, syndiotactic polystyrene (sPS) may possess various combinations of four different unit cell forms (α, β, γ, δ) depending on the thermal history and/or solution treatments [1–4]. Normally, co-existing α and β forms are obtained with melt-processed sPS. The α and β forms are more common and associated with polymer chains in trans-planar (zig-zag) conformation while the γ and δ forms are with a helical conformation [5,6]. In addition, many recent studies point out that melt-crystallization at high temperatures preferentially favors the formation of the β-form [7–10].

Morphology in cold-crystallized sPS has been less studied. Cold-crystallization means crystallization of polymers from a quenched glassy/amorphous state. It has been preliminarily shown that cold-crystallized sPS differs significantly from melt-crystallized sPS in crystal forms and melting behavior [11]. This study is aimed to understand in greater detail the main characteristics of spherulitic or lamellar morphology and the relationship between morphology, unit cell crystal forms, and thermal behavior in cold-crystallized sPS.

2. Experimental

2.1. Materials and procedures

Semicrystalline sPS was obtained as a courtesy sample material from Idemitsu Petrochemical Co., Ltd., Japan, with a medium $M_w = 63{,}000$ g/mol and PI (M_w/M_n) = 2.8 (powder form). DSC characterization revealed that T_g of quenched glassy sPS is 84°C (onset). The grade of sPS used in this study possesses a much lower molecular weight than the earlier study [11]. For cold-crystallization, initially amorphous sPS was prepared as a starting material. Amorphous sPS (free of initial crystallinity) as a starting material was prepared by heating the as-received sPS (powder) to 310°C, compression-molded into a thin film (between two aluminum plate molds), then quickly quenched into liquid nitrogen or iced water. Transparent, crystal-free, amorphous sPS material was obtained upon quenching. The amorphous sPS film was then cut into disks of proper sizes for various thermal treatments (cold-crystallization at designated temperatures for various times). For exact temperature accuracy, all thermal treatments of sPS samples were performed in the cells of the differential scanning calorimeter. Thermal treatments were properly done prior to X-ray diffraction or SEM characterization.

2.2. Apparatus

Differential scanning calorimetry (DSC-7, Perkin–Elmer) was used for determining the melting transition

* Corresponding author. Tel.: +886-6-275-7575 ext. 6270; fax: +886-6-234-4496.

E-mail address: emwoo@mail.ncku.edu.tw (E.M. Woo).

PII: S0032-3861(00)00574-7

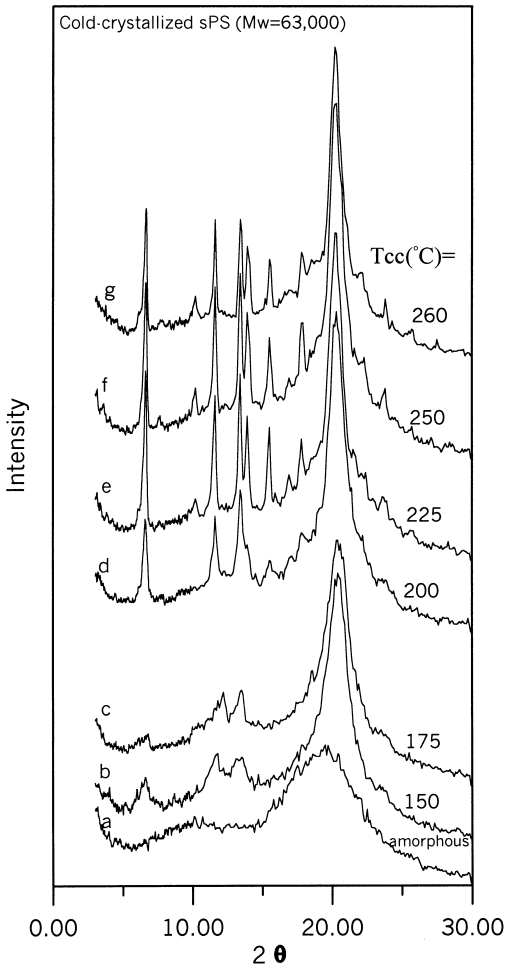

Fig. 1. X-ray diffractograms for (a) amorphous sPS, and sPS samples cold-crystallized at (b) 150, (c) 175, (d) 200, (e) 225, (f) 250, and (g) 260°C for 120 min.

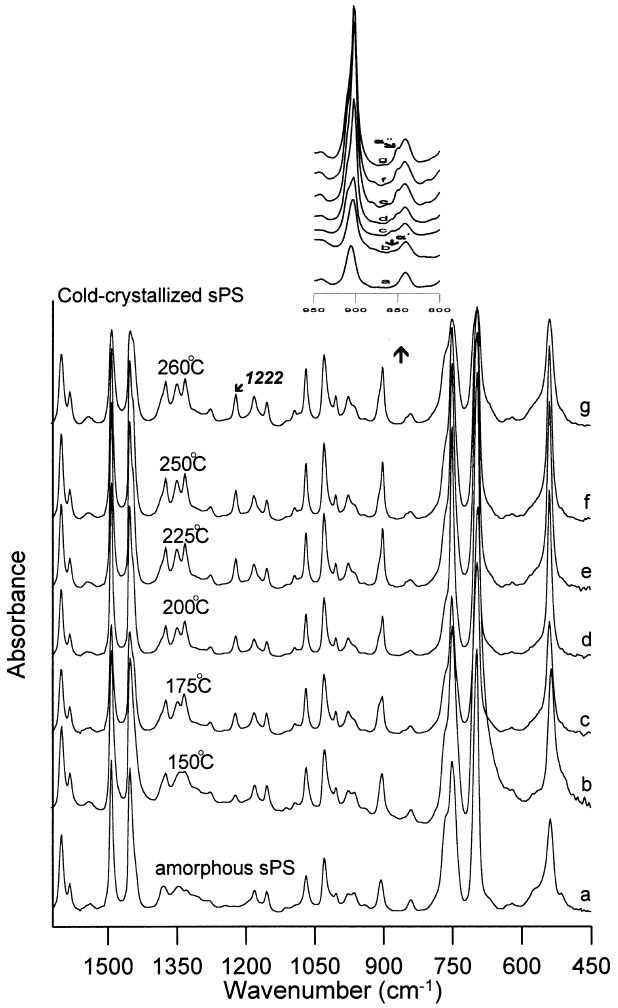

Fig. 2. FT-IR spectra of (a) the quenched sPS (amorphous), and cold-crystallized sPS at (b) 175, (c) 200, (d) 225, and (e) 250°C, all for 120 min.

temperatures and enthalpy of melting peaks. A uniform heating rate of 10°C/min was used in all T_m measurements unless otherwise specified. The instrument was calibrated with indium and zinc standards at 10°C/min on the temperature and heat of the transitions. The spherulitic/lamellar morphology of the samples was examined using a scanning electron microscope (SEM, Philips XL-40 FEG). Etching by 2% potassium permanganate in $H_3PO_4 + H_2SO_4$ (1:2) solution (24 h at ambient) was performed to enhance crystalline/amorphous contrast. The washed/dried samples were then coated with gold by vapor deposition using a vacuum sputter prior to SEM characterization. The X-ray instrument was Rigaku D/Max II-B with copper K_α radiation ($\lambda = 1.542$ Å), which was used for determining the unit-cell packing. Specimens for X-ray characterization were prepared in DSC cells using similar thermal treatments as described for the thermal analysis samples. Fourier-transform infrared spectroscopy (FT-IR, Nicolet Magna-560) was also used for investigating the crystal forms in cold-crystallized sPS. Spectra were obtained at 2 cm^{-1} resolution and averages of spectra were obtained from at least 64 scans in the standard wavenumber range of 400–4000 cm^{-1}. All the samples for FT-IR analysis were molded as thin films sandwiched between two KBr pellets heated at ~300°C. Quenching of the samples was performed by quickly dipping them into liquid nitrogen while the KBr-sandwiched polymer was still in a molten state.

3. Results and discussion

To understand the mechanism of crystal packing and/or lamellar characteristics in cold-crystallized sPS in detail, sPS samples were brought to crystallization from the amorphous/glassy state to several isothermal temperatures: 150, 175, 200, 225, 250, or 260°C. They were brought to cold-crystallization at designated temperatures and quickly stabilized; subsequently, upon completion, they were quenched immediately to ambient. These procedures were crucial for the purpose of avoiding additional crystal formation during the heating or cooling of the transients. Fig. 1(a)–(g) shows X-ray diffractograms

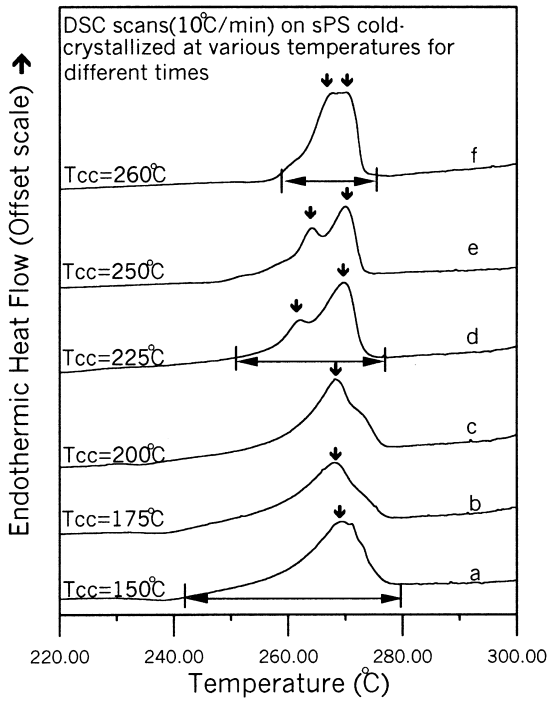

Fig. 3. DSC thermograms for sPS cold-crystallized at isothermal temperatures: (a) 150, (b) 175, (c) 200, (d) 225, (e) 250°C, all for 30 min, and (f) 260°C, for 120 min.

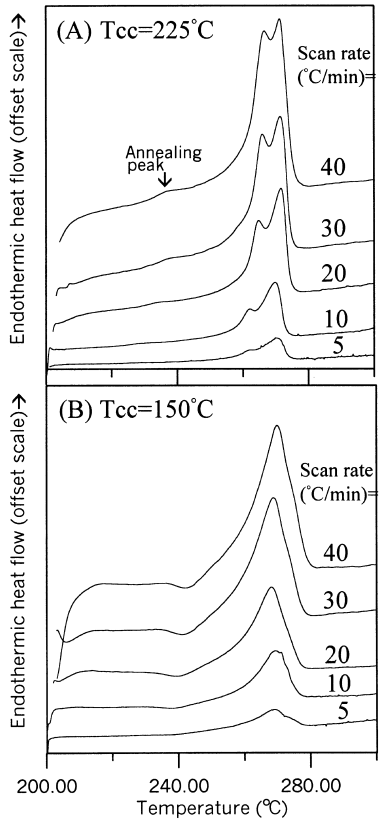

Fig. 4. DSC results (scanning rates 5–40°C/min) on sPS cold-crystallized at (A) 225°C and (B) 150°C.

for (a) amorphous sPS and sPS cold-crystallized at (b) 150, (c) 175, (d) 200, (e) 225, (f) 250, and (g) 260°C for 120 min. Interestingly, only the α-form crystal is present, and all characteristic peaks of the β-crystal ($2\theta = 6.1$, 10.4, 12.3, 13.6, 18.6, 20.2, 21.3 and 23.9°) are absent from the cold-crystallized sPS. Depending on crystallization temperatures, the α-form can be subdivided into two minor forms: α'-crystal at temperatures below 175°C and α''-crystal at temperatures above 200°C. The samples cold-crystallized at lower temperatures (i.e. 150 and 175°C) exhibited three diffraction peaks at $2\theta = 6.7$, 11.8, and 18.0°, which are the α' forms [2]. But the sPS samples cold-crystallized at higher temperatures of 200, 225, 250, or 260°C exhibited sharper diffraction peaks at $2\theta = 6.8$, 10.3, 11.7, 14.0, 15.6, 17.0, and 20.2°, which are typical of α''-crystal [2]. The peak at 20.2° is characteristic of the α and β forms and is present regardless of thermal treatment. The X-ray result indicates that the α-form crystal (hexagonal unit cell) is the dominant crystalline domain in cold-crystallized sPS, with two sub-forms (α'- and α''-crystals), and that high temperatures favor α''-crystal and lower temperatures favor α'-crystal (<175°C).

Fig. 2(a)–(g) displays the FT-IR spectra of (a) the quenched sPS (amorphous) and (b)–(g) cold-crystallized sPS at 150, 175, 200, 225, 250, and 260°C for 120 min, respectively. The absence of the 1222 cm^{-1} peak suggests that this is indeed an amorphous sPS. For the cold-crystallized sPS, a peak at 1222 cm^{-1} was clearly seen, which is associated with α-crystal molecular chain trans-skeletal conformation [12–15]. Spectrum-a reveals a peak at 905.5 cm^{-1} for the amorphous sPS. For the cold-crystallized sPS samples, a sharper peak at 901.7 cm^{-1} (adjacent to the 905.5 cm^{-1} peak) was seen, which is indicative of α-crystals. Additionally, for the sPS cold-crystallized at 200°C, there are two small but distinct peaks located at 856.8 and 852 cm^{-1}, respectively, indicating α'- and α''-crystals [12–15]. The IR result confirmed that only the α-crystal (α'- and α''-crystals) was found in the cold-crystallized sPS. This confirms that the α'-crystal was favored at lower-temperature cold-crystallization (175°C), but a combination of α'- and α''-crystals co-existed at medium temperatures (200°C). Only the α''-crystal was obtained when cold-crystallized at higher temperatures above 225°C.

DSC analysis was then performed to reveal the thermal characteristics of cold-crystallized sPS. Fig. 3 shows DSC thermograms (a)–(f) for sPS cold-crystallized at isothermal temperatures: (a) 150, (b) 175, (c) 200, (d) 225, (e) 250°C, all for 30 min, and (f) 260°C for 120 min. Evidently, the thermal behavior as seen in the DSC thermograms exhibits a continuous trend of variation depending on the temperature of cold-crystallization imposed on the samples. In general, as the cold-crystallization temperature increases, the breadth of the melting peaks (as indicated by the double-arrow range) decreases. A rather broad endothermic melting peak is observed when crystallized at 150–200°C.

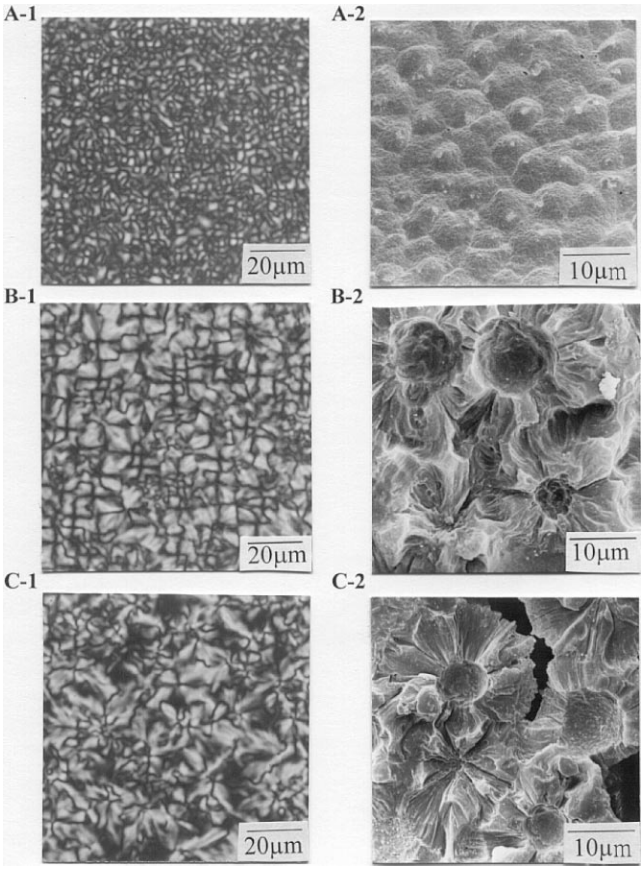

Fig. 5. POM and SEM graphs, respectively, for sPS samples: (A-1&2) cold-crystallized at low $T_{cc} = 150$°C, (B-1&2) cold-crystallized at $T_{cc} = 225$°C, all for 120 min, and (C-1&2) cold-crystallized at $T_{cc} = 260$°C, all for 120 min.

Further, the melting behavior of the crystals in sPS cold-crystallized at higher temperatures (225–260°C) is seen to be significantly different from the sPS sample cold-crystallized at 150°C. First, the samples crystallized at temperatures between 175 and 200°C exhibit a broad melting peak superimposed with a minor but sharper shoulder endothermic peak. At higher temperatures of cold-crystallization, the sharper peak rapidly shifts to a higher temperature. For the sPS cold-crystallized at 260°C, the sharp shoulder peak is almost overlapped with the peak of the broad endotherm. This phenomenon may be due to other lamella developed in sPS cold-crystallized at higher temperatures above 225°C.

DSC runs at different rates were performed on sPS samples cold-crystallized at low and high temperatures. Fig. 4(A) and (B) shows the DSC results (scanning rates 5–40°C/min) on sPS cold-crystallized at (A) 225°C and (B) 150°C. For the sPS samples cold-crystallized at 225°C, the samples exhibited dual sharp melting peaks. The dual melting peaks were not considered as a result of melting/reorganization. If the reorganization mechanism had been correct in this case, the intensity of the higher melting peak (268–270°C) would have been diminished and the position of the higher melting peak shifted to a lower temperature upon scanning at higher rates, which is not the case. For the sPS cold-crystallized at 150°C, all samples exhibited a similar breadth of melting range regardless of scanning rates. It was thus difficult to assess whether re-organization was responsible. It is likely, but no direct evidence could be obtained.

A more revealing difference in morphology was found on examining the lamellar structure by using POM and SEM. For direct comparison, the POM and SEM results are placed side by side. Fig. 5 shows the POM and SEM morphology for the sPS samples of different thermal treatments: (A-1&2) cold-crystallized at 150°C, in comparison with (B-1&2) cold-crystallized at 225°C, and (C-1&2) cold-crystallized at 260°C, all for 120 min. The optical graph (A-1) shows tiny granular structures in sPS cold-crystallized at a low temperature of 150°C. Graph A-2 shows the morphology in sPS cold-crystallized at 150°C revealing small granular crystallites of less than 80 nm. Unlike regular spherulites grown from the molten state, no bundles of lamellae were found (or visible) inside the granular spheres of cold-crystallized sPS. Thus, cold-crystallization (at 150°C) yielded a unique morphology of aggregation of many tiny underdeveloped spherulites, which may be due to higher nucleation rates and lower molecular mobility during lower crystallization temperature. At low temperatures, the high nucleation rate means that many nuclei develop at the same instant, thus leaving less material for later lamellar growth. On the other hand, Graphs B-1&2 show that post-development of lamellar morphology surrounding the tiny spheres was observed if the sPS was cold-crystallized at increasingly higher temperatures (225, 260°C). The POM graph (B-1) shows that when cold-crystallized at the higher temperatures of 225 or 260°C, only lamellar structures were visible, lacking a spherulitic birefringence pattern. The SEM graphs (B-2 and C-2) show that sPS, cold-crystallized at 225 or 260°C for 120 min, developed a peculiar morphology consisting of tiny crystals in the spherical center with secondary lamellae radiating out from the spheres.

If one combines the results of POM, SEM, FT-IR, and DSC analyses, interesting clues can be found. The additional peak (the lower one of the twin peaks) found in sPS cold-crystallized at temperatures higher than 225°C is possibly associated with the melting of sheaf-like lamellar bundles (which radiate out from the central tiny spheres or spherulites). The sheaf-like lamellae possess a relatively narrow thickness distribution, as judged from the sharp melting peak. The radiating lamellae outside the spheres can be thickened more readily when held at higher temperatures (225–260°C), which was evidenced by the experimental observation that higher cold-crystallization temperature led to an elevating peak temperature. By comparison, possibly owing to geometric constraints, the broad-distributed lamella inside the granular spheres cannot be thickened (as a population) with respect to higher temperatures as easily as the sheaf-like lamella grown outside the small

granular spheres. The granular spheres contain a broad lamellar distribution of various thicknesses (with the peak of the broad melting endotherm at ca. 268°C regardless of the temperature of cold-crystallization. It must be emphasized here that sPS, originally cold-crystallized at low temperatures. (150–200) and subsequently scanned to high temperatures (such as 225–260°C), did not produce the sheaf-like lamellae. Only sPS directly subjected to high-temperature cold-crystallization (at 225–260°C) produced additional sheaf-like lamella radiating out from the central spheres.

4. Conclusions

Cold-crystallization of sPS ($M_w = 63{,}000$ g/mol produced only α-type unit cell, packed to form two major crystalline domains of different lamellar morphologies depending on temperatures. The α-type unit cell crystal in cold-crystallized sPS is consistent with earlier studies [11] on sPS of higher molecular weights ($M_w = 240{,}000$ g/mol). The spherulite morphology of α-cell sPS contains a tiny granular-sphere texture when cold-crystallized at low temperatures; however, high-temperature cold-crystallization produced additional sheaf-like lamella radiating out from the central granular spheres.

The thermal behavior, lamellar morphology, and correlations between melting and different lamellae in the cold-crystallized α-cell sPS were also investigated. The tiny granular spherulites, produced in low-temperature cold-crystallization, yielded a broad melting endotherm with the peak temperature remaining almost constant at 268–270°C, which may be attributed to roughly similar lamellae thickness distribution in the tiny spherulites regardless of the temperature of cold-crystallization. On the other hand, the sheaf-like lamella (radiating outside the spheres) produced in high-temperature cold-crystallization yielded a rather sharp melting peak superimposed on the original broad melting peak.

Acknowledgements

The work was supported by research grants from Taiwan's National Science Council (#NSC89 2216 E006 014). The authors are grateful to Mr Masahiko Kuramoto of Idemitsu Petrochemicals Co. Ltd, Japan, who kindly supplied the research-grade sPS material. This paper has benefited a great deal from the expert comments made by the reviewers, whose suggestions have been incorporated and to whom the authors express their most sincere gratitude.

References

[1] Tosaka M, Tsuji M, Cartier L, Lotz B, Kohjiya S, Ogawa T, Isoda S, Kobayashi T. Polymer 1998;39:5273.
[2] Guerra G, Vitagliano VM, De Rosa C, Petraccone V, Corradini P. Macromolecules 1990;23:1539.
[3] De Rosa C, Rapacciuolo M, Guerra G, Petraccone V, Corradini P. Polymer 1992;33:1423.
[4] De Rosa C. Macromolecules 1996;29:8460.
[5] Sun Z, Morgan RJ, Lewis DN. Polymer 1992;33:660.
[6] Chatani Y, Shimane Y, Ijitsu T, Yukinari T. Polymer 1993;34:1625.
[7] Vittoria V, Ruvolo Filho A, De Candia F. J Macromol Sci, Phys 1992;B31:133.
[8] Woo EM, Wu FS. Macromol Chem. Phys 1998;199:2041.
[9] Evans AM, Kellar EJC, Knowles J, Galiotis C, Carriere CJ, Andrews EH. Polym Engng Sci 1997;37:153.
[10] Sun YS, Woo EM. Macromolecules 1999;32:7836.
[11] Woo EM, Sun YS, Lee ML. Polymer 1999;40:4425.
[12] Zimba CG, Rabolt JF, English AD. Macromolecules 1989;22:2867.
[13] Musto P, Tavone S, Guerra G, De Rosa C. J Polym Sci, Part B: Polym Phys 1997;35:1055.
[14] Vittoria V. Polym Commun 1990;31:263.
[15] Reynolds NM, Stidham HD, Hsu SL. Macromolecules 1991;24:3662.